

1 **Snowball Earths, population bottlenecks, and the evolution of marine**  
2 **photosynthetic bacteria**

3 Hao Zhang<sup>1^</sup>, Ying Sun<sup>1^</sup>, Qinglu Zeng<sup>2</sup>, Sean A. Crowe<sup>3</sup>, Haiwei Luo<sup>1\*</sup>

4

5 <sup>1</sup>Simon F. S. Li Marine Science Laboratory, School of Life Sciences and State Key  
6 Laboratory of Agrobiotechnology, The Chinese University of Hong Kong, Shatin, Hong  
7 Kong SAR

8 <sup>2</sup>Department of Ocean Science, The Hong Kong University of Science and Technology,  
9 Clear Water Bay, Hong Kong SAR

10 <sup>3</sup>Department of Earth Sciences, School of Biological Sciences, and Swire Institute for  
11 Marine Science (SWIMS), University of Hong Kong, Pokfulam Road, Hong Kong SAR

12 <sup>^</sup>These authors contributed equally to this study.

13

14 **\*Corresponding author:**

15 Haiwei Luo

16 The Chinese University of Hong Kong

17 Shatin, Hong Kong SAR

18 Phone: (+852) 39436121

19 E-mail: hluo2006@gmail.com

20

21 **Running Title:** *Prochlorococcus* and Snowball Earths

22 **Keywords:** *Prochlorococcus*, Neoproterozoic Snowball Earth, genome reduction,  
23 molecular dating.

24

25

26 **Abstract**

27 *Prochlorococcus* are the most abundant photosynthetic organisms in the modern ocean. A  
28 massive DNA loss event occurred in their early evolutionary history, leading to highly  
29 reduced genomes in nearly all lineages, as well as enhanced efficiency in both nutrient  
30 uptake and light absorption. The environmental landscape that shaped this ancient  
31 genome reduction, however, remained unknown. Through careful molecular clock  
32 analyses, we established that this *Prochlorococcus* genome reduction occurred during the  
33 Neoproterozoic Snowball Earth climate catastrophe. The lethally low temperature and  
34 exceedingly dim light during the Snowball Earth event would have inhibited  
35 *Prochlorococcus* growth and proliferation and caused severe population bottlenecks.  
36 These bottlenecks are recorded as an excess of deleterious mutations that accumulated  
37 across genomic regions in the descendant lineages. *Prochlorococcus* adaptation to  
38 extreme environmental conditions during Snowball Earth intervals can be inferred by  
39 tracing the evolutionary paths of genes that encode key metabolic potential. This  
40 metabolic potential includes modified lipopolysaccharide structure, strengthened  
41 peptidoglycan biosynthesis, the replacement of a sophisticated circadian clock with an  
42 hourglass-like mechanism that resets daily for dim light adaption, and the adoption of  
43 ammonia diffusion as an efficient membrane transporter-independent mode of nitrogen  
44 acquisition. In this way, the Neoproterozoic Snowball Earth event altered the  
45 physiological characters of *Prochlorococcus*, shaping their ecologically vital role as the  
46 most abundant primary producers in the modern oceans.

## 47 **Introduction**

48 *Prochlorococcus* are the smallest and most abundant photosynthetic organisms on  
49 Earth<sup>1</sup>. They are prevalent throughout the photic zone of the oligotrophic oceans between  
50 40°N and 40°S<sup>1</sup>, where they account for more than 40% of the biomass and contribute  
51 almost half of the net primary production<sup>2</sup>. *Prochlorococcus* have diversified into two  
52 major phylogenetic groups with distinct ecology (ecotypes), with the high-light (HL)  
53 adapted monophyletic group imbedded in the low-light (LL) adapted paraphyletic group<sup>3</sup>.  
54 The distinct ecotypes of *Prochlorococcus* evolved different pigments, light-harvesting  
55 systems, and the phycobiliproteins, which allowed for efficient light absorption in the  
56 water column<sup>4</sup>, and thus increased growth rates and primary production<sup>5</sup>.

57 *Prochlorococcus* genomes have been shaped by stepwise streamlining, including a  
58 major genome reduction in their early evolution and a few minor modifications that  
59 followed<sup>6,7</sup>. Modern marine *Prochlorococcus* lineages, in particular those with small  
60 genomes, show very low ratios of nonsynonymous ( $d_N$ ) to synonymous ( $d_S$ ) nucleotide  
61 substitution rates, suggesting that natural selection is a highly efficient throttle on the  
62 accumulation of deleterious mutations (i.e., nonsynonymous mutations) in  
63 *Prochlorococcus*<sup>6,8</sup>. On long time scales, however, nucleotide substitutions at  
64 synonymous sites become saturated, invalidating the use of  $d_N/d_S$  to infer selection  
65 efficiency in deep time<sup>9</sup>. Thus, an alternative approach focuses instead on different types  
66 of nonsynonymous substitutions leading to radical versus conservative changes in amino  
67 acid sequences, with the former more likely to be deleterious<sup>10,11</sup>. Excess radical  
68 mutations accumulate from random fixation of deleterious mutations by genetic drift (i.e.,  
69 reduced efficiency of selection). Using this approach reveals that the major genome

70 reduction in *Prochlorococcus* took place under reduced selection efficiency<sup>9</sup> and implies  
71 that the ancient population went through severe bottlenecks as the likely result of  
72 environmental catastrophe.

73 The environmental context underlying *Prochlorococcus* genome reduction remains  
74 unknown, however, and precise molecular dating is needed to link this important  
75 evolutionary event to its possible environmental drivers. Implementing comprehensive  
76 molecular clock analyses, we now link the early major genome reduction event of  
77 *Prochlorococcus* to the Neoproterozoic Snowball Earth events. These catastrophic  
78 disruptions to the Earth system would likely have challenged warm-water-loving  
79 photosynthetic *Prochlorococcus*, with strong potential to cause the population  
80 bottlenecks inferred from the genome sequences described above. *Prochlorococcus*  
81 survived this catastrophe through likely gains and losses of key metabolic functions  
82 reconstructed from the same genome sequences, which have far-reaching impact on their  
83 success in today's oceans. *Prochlorococcus* are thus vital “guardians of metabolism”<sup>12</sup>,  
84 shepherding genes critical to the functioning of the biosphere across environmental  
85 catastrophes, including global glaciations.

## 86 **Results and Discussion**

87 *Prochlorococcus* experienced a massive gene loss event on the ancestral branch  
88 leading to the last common ancestor (LCA) of clades HL, LLI and LLII/III<sup>6,7,13</sup>. This is  
89 confirmed by our analysis, which reconstructed 366 and 107 gene family losses and gains  
90 on this branch, respectively (Fig. 1A & S1), among which 163 and 84 encode unknown  
91 proteins. On the same ancestral branch, it was shown that  $d_R/d_C$  is significantly elevated  
92 compared to the sister ancestral branch leading to the LCA of the LLIV<sup>9</sup>, which was

93 validated here (both sign test and paired  $t$ -test,  $p < 0.001$ ; Fig. 1B). These results confirm  
94 that the major genome reduction event occurring on this branch was likely driven by  
95 genetic drift as a result of one or recurrent population bottlenecks<sup>9</sup>. Given the global  
96 distribution and abundance of *Prochlorococcus*, and cyanobacteria more generally, such  
97 a bottleneck would likely require a global-scale event, like an environmental or climate  
98 catastrophe (e.g. meteorite impact, large igneous province emplacement, or glaciation).

99 To establish the environmental context for the large, ancient genome reduction, we  
100 estimated the timeline of *Prochlorococcus* evolution by implementing molecular clock  
101 analyses based on essential calibrations available in the cyanobacterial lineage. We  
102 recognize that the use of calibration sets adapted from previous studies (under  
103 calibrations C1-C6 in Table S1 with related references included there) results in up to  
104 ~320 Ma disparity (Fig. S2A) in the estimated time for the LCA of *Prochlorococcus* HL,  
105 LLI and LLII/III clades that emerged with the major genome reduction. We note that the  
106 calibrations in previous studies were not properly used. For example, the akinete fossil  
107 identified to 2,100 Mya was used as either the maximum bound or the minimum bound to  
108 calibrate the crown group of Nostocales<sup>14,15</sup>. However, given the fact that apomorphic  
109 character must evolve earlier than the divergence of crown group, morphological fossils  
110 can only serve as the minimum bounds on total groups of assigned lineages<sup>16</sup> (see Section  
111 2.3 in Supplemental Methods for details). Thus, in the present study, we modified the  
112 calibration sets by constraining the lower bounds of the Nostocales (and the  
113 Pleurocapsales) total groups with morphological fossils and by leaving their upper  
114 bounds open (C9-C14; Table S1). Intriguingly, the variation is reduced to less than 10 Ma  
115 when these modified calibration sets are used (Fig. S2A).

116 Recent identification of non-oxygenic Cyanobacteria lineages such as  
117 Melainabacteria and Sericytochromatia as sister groups of oxygenic Cyanobacteria<sup>17,18</sup>  
118 provides an alternative way to constrain the evolution of oxygenic Cyanobacteria.  
119 Specifically, given that oxygenic photosynthesis evolved at the stem lineage of oxygenic  
120 Cyanobacteria, we constrained the minimum age of total Cyanobacteria group at 3.0 Ga,  
121 which is supported by geochemical evidence as the time when atmospheric oxygen  
122 became available<sup>38,56</sup>. To avoid the overly precise and potentially misleading age  
123 estimates, we calibrated the upper limit of the Cyanobacteria root using the ages when the  
124 planet Earth formed and became habitable (C15-C38 in Table S1; see Section 2.3 in  
125 Supplemental Methods for details). Using this strategy, we show that the age of  
126 *Prochlorococcus* major genome reduction remains stable when non-oxygenic  
127 Cyanobacteria outgroups were included (Fig. S2B). Since including the non-oxygenic  
128 Cyanobacteria have consistently reduced the precision of posterior age estimates,  
129 manifested as the higher slopes of the regression line between HPD width and the  
130 posterior age estimates compared to those without including these lineages (C15-C38  
131 versus C1-C14 in Fig. S3; also see Section 2.6 in Supplemental Methods for extended  
132 discussion), we focus on the crown oxygenic Cyanobacteria group dating (C7-C14) in the  
133 following discussions.

134 By comparing the width of the 95% highest posterior density (HPD) derived from  
135 each molecular clock analysis (Fig. S3), we inferred the most precise timeline of  
136 *Prochlorococcus* evolution (corresponding to calibration set C14 in Table S1; see Section  
137 2.3 in Supplemental Methods). Our time estimates revealed that the LCA of  
138 *Prochlorococcus* HL, LLI and LLII/III clades diversified at 682 Mya [95% HPD

139 (=highest posterior density) 632-732 Mya], precisely dating the genome reduction event  
140 to this time. A 682 Mya date for the emergence of the LCA of *Prochlorococcus* HL, LLI  
141 and LLII/III clades places the large genome reduction that took place in this lineage  
142 firmly within the Cryogenian Period (~720 to 635 Mya; Fig. 1A) and implicates the  
143 Snowball Earth icehouse climate conditions eponymous with the Period in the  
144 corresponding *Prochlorococcus* population bottleneck. We therefore refer to this ancestor  
145 as SBE-LCA (see Fig. 1A), short for “Snowball Earth” LCA. The Neoproterozoic climate  
146 catastrophe culminated in the Sturtian (~717 to 659 Mya) and Marinoan (~645 to 635  
147 Mya) glaciations (Fig. 1A), which stretched from the poles to sea level near the equators,  
148 possibly wrapping the entire Earth under a frozen skin<sup>19</sup>. This “Snowball Earth” persisted  
149 with the freezing temperature of seawater below the ice sheet lowered to -3.5 °C<sup>20</sup>. Since  
150 all assayed *Prochlorococcus* strains, including those affiliated with the basal LL  
151 ecotypes, reach maximum growth rates at approximately 25 °C and rarely survive when  
152 temperature drops to ~10 °C (Fig. 1C)<sup>21</sup>, we propose that extreme climate cooling during  
153 the Neoproterozoic Snowball Earth events was likely the major driver of severe  
154 bottlenecks in early *Prochlorococcus* populations.

155 Survival of *Prochlorococcus* populations through the Cryogenian would have  
156 required refugia, the nature of which would have shaped continued *Prochlorococcus*  
157 evolution. A variety of biotic refugia have been identified during Snowball Earth  
158 intervals, including the sea-ice brine channels within ice grounding-line crack systems<sup>22</sup>  
159 and cryoconite holes/ponds on the surface of the sublimation zone, which may have  
160 represented ~12% of the global sea glacier surface<sup>23</sup> (Fig. 1D). Despite providing the  
161 essential space for *Prochlorococcus* survival, these refugia would have presented a

162 number of environmental stresses to *Prochlorococcus* populations including: low  
163 temperature, low light, high and variable osmotic pressure, and limited nutrients<sup>22-24</sup>.  
164 *Prochlorococcus* thus evolved a number of adaptive mechanisms to cope with these  
165 stresses via gene gains and losses, which we assessed by reconstructing the evolutionary  
166 paths of imprints that the Snowball Earth climate left in extant *Prochlorococcus*  
167 genomes.

168       Among these stresses, the most prominent was likely lethally low temperature.  
169 Maintaining membrane fluidity is of paramount importance under low temperature  
170 conditions, which is largely achieved by the activities of fatty acid desaturase encoded by  
171 *desA* and *desC*. As a result, we inferred that these genes were retained in SBE-LCA (Fig.  
172 1A). Lipopolysaccharide (LPS) in the outer membrane is known to provide the first line  
173 of defense against harsh environments<sup>25</sup>, which contains the O-specific polysaccharide,  
174 the glycolipid anchor lipid A, and the polysaccharide core region. Based on our analyses,  
175 genes encoding the polysaccharide core region (*kdsABCD* for 3-deoxy-d-manno-  
176 octulosonate biosynthesis; Fig. 1A) were likely lost at SBE-LCA, while those encoding  
177 the other components were retained (*lpxABCD* and *rfbABC* for Lipid A precursor and O-  
178 specific LPS precursor biosynthesis; Fig. 1A). This inference is consistent with a  
179 previous conclusion that the loss of the LPS core region would increase the  
180 hydrophobicity and permeability of the cell envelope<sup>26</sup> to protect against the cold  
181 conditions<sup>27</sup>. The amino sugar N-acetylglucosamine (GlcNAc) is used by bacteria such as  
182 *Corynebacterium glutamicum* as a carbon, energy and nitrogen source<sup>28</sup>. GlcNAc enters  
183 bacteria in the form of GlcNAc-6-phosphate (GlcNAc-6-P). However, instead of being  
184 metabolized, the loss of *nagB* for GlcNAc-6-P deamination at SBE-LCA suggests that



185 GlcN6P is more likely to be involved in peptidoglycan (PG) recycling through the  
186 cascade catalysis by GlmM and GlmU (Fig. 1A) to generate UDP-GlcNAc, which is an  
187 essential precursor of cell wall PG and LPS<sup>29</sup>. During cell turnovers, PG is continuously  
188 broken down and reused through the PG recycling pathway to produce new PG, and in  
189 some bacteria, PG recycling is critical for their long-term survival when growth is stalled  
190 under nutrient limitation<sup>30</sup>. Thus, such a recycling mechanism seems to be key for  
191 maintenance of cell integrity in SBE-LCA under oligotrophic and lethally freezing  
192 conditions<sup>23</sup>. Another metabolic modification in SBE-LCA was related to heat shock  
193 proteins (HSPs), which play crucial roles in tolerating environmental stresses including  
194 thermal shocks. Typically, HSPs are tightly regulated, as they respond quickly to stress  
195 and turn off rapidly once the stress disappears<sup>31</sup>. However, the HSP repressor protein  
196 encoded by *hrcA* was inferred to be lost at SBE-LCA, which thus likely allowed the  
197 organism to continuously express HSPs to cope with prolonged lethally low temperature.  
198 In fact, constitutive expression of HSPs occurs in polar organisms such as the Antarctic  
199 ciliate *Euplotes focardii*<sup>32</sup> and the polar insect *Belgica antarctica* larvae<sup>33</sup>. Extremely low  
200 temperature also made substrate acquisition difficult due to increased lipid stiffness and  
201 decreased efficiency and affinity of membrane transporters<sup>34</sup>. Under such conditions,  
202 bacteria may increasingly rely on substrates whose uptake shows lower dependence on  
203 temperature. In sea-ice brines where less CO<sub>2</sub> is dissolved<sup>35</sup>, elevated pH promotes the  
204 conversion of ammonium to ammonia, which diffuses directly into cells without the aid  
205 of transporters in the membrane. Accordingly, species of bacteria and microalgae show a  
206 greater dependence on ammonium and ammonia at low temperatures and high pH than  
207 nitrate<sup>36,37</sup>, thereby reducing reliance on membrane transporters. In SBE-LCA, the

208 potentially efficient utilization of ammonia made other N acquisition genes dispensable,  
209 leading to the neutral loss of nitrite transporter (*nitM*), whereas glutamine synthetase  
210 (*glnA*) and glutamate synthase (*gltS*) responsible for the utilization of ammonia after its  
211 assimilation were conserved (Fig. 1A).

212 An additional stress to *Prochlorococcus* during Snowball Earth would have been  
213 variable osmotic pressure. Although multiple refugia might have supported bacterial  
214 survival during Snowball Earth, the schizohaline nature of these refugia must have  
215 imposed strong osmotic pressure on ice-trapped bacteria<sup>23</sup>. As temperature dropped, salts  
216 would have become increasingly concentrated in brine channels<sup>22</sup>, whereas cryoconite  
217 ponds would have remained hyposaline, similar to modern Arctic and Antarctic  
218 cryoconite ecosystems<sup>38</sup>. Glycine betaine (GB) is among the most important organic  
219 osmolytes in halophilic cyanobacteria, and is used as the major osmolyte in  
220 *Synechococcus* sp. WH8102<sup>39</sup>. However, genes involved in glycine betaine biosynthesis  
221 and transport were lost at SBE-LCA, including *bsmB* for dimethylglycine N-  
222 methyltransferase, *gsmt* for glycine/sarcosine N-methyltransferase, and *proVWXP* for  
223 glycine betaine/proline transport system (Fig. 1A). Instead, several other organic  
224 osmolytes might have been used during the Snowball Earth, as their biosynthetic genes  
225 were retained at SBE-LCA. The first examples are the *ggpS* gene encoding  
226 glucosylglycerol phosphate synthase for glucosylglycerol (GG) synthesis and the *gpgS*  
227 encoding glucosyl-phosphoglycerate synthase for glucosylglycerate (GGA) synthesis  
228 (Fig. 1A). GG and GGA may be sufficient to provide osmotic tolerance under moderately  
229 saline conditions<sup>40</sup>. Interestingly, the biosynthesis of GG and GGA requires less N  
230 compared to that of GB<sup>40,41</sup>, and thus the potential use of GG/GGA instead of GB

231 appeared favorable to SBE-LCA, which had a reduced efficiency of membrane  
232 transporters and a low affinity for external nutrients at exceedingly low temperature.  
233 Low light intensity during Snowball Earth was another formidable challenge to  
234 phototrophs including *Prochlorococcus*. In the Neoproterozoic, the Sun was still at least  
235 6% dimmer than that at present<sup>42</sup>. Moreover, sea ice, especially when covered with snow,  
236 is an effective barrier to light transmission<sup>43</sup>. This is in analogy to the deeper layers of  
237 today's polar snow and glacier ice where irradiation is reduced and photosynthetic  
238 organisms and activities are scarcely detectable<sup>44</sup>. Consequently, photosynthetic  
239 organisms trapped in the brine channels or inhabiting waters below ice need to be  
240 physiologically geared to cope with low light. It was proposed that modification of the  
241 photosystem structure enables adaptation to the low light condition<sup>45</sup>. We inferred a few  
242 changes in photosystem I and II (PSI/PSII) that occurred in SBE-LCA, including the gain  
243 of RC1 subunit PsaM, RC2 subunit PsbY, and an extra copy of the RC2 subunit PsbF, the  
244 loss of RC2 protein PsbU, and the replacement of RC2 subunit PsbX (Fig. 1A), but the  
245 molecular mechanism of these changes underlying low light adaptation is poorly  
246 understood. We also inferred an expansion of the *Prochlorococcus* antenna Pcb from two  
247 to six copies during the Snowball Earth (Fig. 1A), which may boost the light-harvesting  
248 capacity under low-light conditions<sup>46</sup>.

249 Many cyanobacteria have a sophisticated circadian clock, which is essential in  
250 controlling global diel transcriptional activities of the cells. This circadian oscillator  
251 system requires only three components: KaiA, KaiB and KaiC<sup>47</sup>. While all marine  
252 *Synechococcus* possess the three *kai* genes, most *Prochlorococcus* lack *kaiA* and, as a  
253 consequence, their circadian clocks rather behave like an “hourglass” which is reset every

254 morning<sup>48-50</sup>. Our analysis indicated that *kaiA* was lost at SBE-LCA (Fig. 1A). This is  
255 likely due to the prolonged darkness or low light conditions during the Snowball Earth,  
256 rendering the sophisticated circadian clock dispensable.

257 We argue that the genome reduction and metabolic adaptation events discussed  
258 above not only enabled *Prochlorococcus* to survive the Snowball Earth climate  
259 catastrophe, but also shaped the physiological characters and the biogeographic  
260 distribution of their descendants in the modern ocean. For example, the genome reduction  
261 that occurred in the early evolution of *Prochlorococcus* likely resulted in the reduced cell  
262 size and increased surface-to-volume ratio in their descendants, which may have  
263 enhanced their efficiency in nutrient acquisition<sup>51</sup> and eventually led them to dominate  
264 the photosynthetic communities in the most oligotrophic regions of today's oceans<sup>2</sup>.  
265 Likewise, new metabolic strategies that *Prochlorococcus* evolved to overcome the  
266 nutrient stresses during Snowball Earth, such as the recycling of cell wall components  
267 and the use of GG and GGA instead of nitrogen-rich GB as the organic osmolytes,  
268 decreased the nutrient requirements of the descendants' cells and thus contributed to their  
269 success in the modern oligotrophic nitrogen-limited oceans. On the other hand,  
270 modifications of some important metabolic pathways may also have imposed deleterious  
271 effects on *Prochlorococcus* descendants. For example, whereas the replacement of  
272 circadian clock with an hourglass-like mechanism might have facilitated the ancestral  
273 lineage to adapt to the prolonged dim light condition during the Snowball Earth  
274 catastrophe, it likely prevents the dispersal of *Prochlorococcus* to high latitude regions in  
275 the modern ocean, where the day length varies substantially across seasons. Normally,  
276 organisms with circadian rhythms deal with these changes by anticipating the changes of

277 light intensity and promptly regulating cellular processes such as DNA transcription and  
278 recombination via chromosome compaction, a known mechanism to protect DNA from  
279 UV radiation<sup>52,53</sup>. In the absence of the circadian clock, however, species such as  
280 *Prochlorococcus* cannot synchronize the endogenous oscillation with the environmental  
281 cycles and thus are under high risks of cell damages<sup>54</sup>.

## 282 **Concluding Remarks**

283 The Neoproterozoic Snowball Earth hypothesis was proposed decades ago, which  
284 claimed the entire extinction of the photosynthetic organisms<sup>19</sup>. In contrast to the original  
285 “hard” version of the hypothesis, a modified “soft” version of the Snowball Earth  
286 hypothesis was later proposed to include the likely persistence of refugia across the  
287 Cryogenian Period, which allowed for the survival of bacterial and simple eukaryotic  
288 lineages<sup>55,56</sup>. Survivors of the Snowball Earth included photosynthetic  
289 microorganisms<sup>57,58</sup>, which enabled continuous primary production across the  
290 interval<sup>55,59</sup>. Like other autotrophic organisms at the base of a food web, the survival of  
291 *Prochlorococcus* was likely important in sustaining primary production, heterotrophy and  
292 carbon cycling, as well as broader ecosystem functioning during the Snowball Earth  
293 glaciations<sup>55</sup>.

294 On the other extreme, a few studies have proposed that microbial communities might  
295 have been only mildly affected by the Snowball Earth climate catastrophe<sup>58,59</sup>. These  
296 inferences were based on the microfossil and biomarker records, which, due to the lack of  
297 lineage-specificity, did not capture the nuances required to reconstruct effects on many  
298 ecologically important lineages like the *Prochlorococcus* studied here. Instead, we find  
299 that substantial disruptions to the Earth system, like the Neoproterozoic Snowball Earth,

300 leave indelible signatures in microbial genomes, such that these heritable changes allow  
301 us to reconstruct interactions between environmental change and biological evolution  
302 deep in Earth's history. By employing the accelerated genome-wide accumulation of the  
303 deleterious type mutations as a proxy for a rapid decrease in the population size of  
304 ancient lineages, we uncovered severe bottlenecks that shaped the early evolution of  
305 *Prochlorococcus* lineages. The precise molecular clock analyses as well as the ancestral  
306 genome reconstruction, furthermore, enabled us to link dynamics in ancestral population  
307 sizes to changes in metabolic potential and adaptation to icehouse climates through  
308 natural selection. Collectively, our findings demonstrate how paleomicrontological  
309 approaches can be used to connect large-scale dynamics in the Earth System to the  
310 genomic imprints left on extant microorganisms, which shape their ecological role and  
311 biogeographic distribution in the world today. They also illustrate how *Prochlorococci*  
312 acted as important “guardians of metabolism”<sup>12</sup>, safeguarding photosynthetic metabolic  
313 potential across the Snowball Earth climate catastrophe.

## 314 **Materials and Methods**

315 Genomic sequences of Cyanobacteria were downloaded from public databases and  
316 manually annotated (Table S2; see Section 1 in Supplemental Methods). Divergence time  
317 of *Prochlorococcus* was estimated with MCMCTree v4.9e<sup>60</sup> on top of 27 genes (Table  
318 S3) previously proposed to be valuable to date bacterial divergence<sup>61</sup> and *Cyanobacteria*  
319 phylogenomic trees. In previous studies, the LPP (*Leptolyngbya*, *Plectonema* and  
320 *Phormidium*) group of *Cyanobacteria* located either at the basal of the  
321 Microcyanobacteria group<sup>14,62</sup> or at the basal of the Macrocyano bacteria group<sup>63,64</sup>. Our

322 analysis showed that this controversy is likely caused by the inclusion of composition-  
323 heterogeneous proteins, and that using composition-homogeneous proteins led to  
324 consistent support for the former hypothesis (Fig. S4; Table S4; see Section 2.2 in  
325 Supplemental Methods). Since molecular dating analysis is known to be intrinsically  
326 associated with calibration points<sup>65</sup>, we summarized the calibrations of Cyanobacteria  
327 used in previous studies, and modified them for our own analyses with caution.  
328 Moreover, we proposed a new strategy to use calibrations when non-oxygenic  
329 Cyanobacteria were used as outgroups (Table S1; see Section 2.3 in Supplemental  
330 Methods for justification). We further assessed the fitness of different molecular clock  
331 models implemented in MCMCTree by using the package “mcmc3r” v0.3.2, based on  
332 which we decided to use the independent rates model for further molecular clock  
333 analyses. For each molecular clock analysis, the software ran twice with a burn-in of  
334 50,000 and a total of 500,000 generations. The convergence was assessed based on the  
335 correlations of posterior mean time of all ancestral nodes between independent runs (Fig.  
336 S5). By implementing statistical tests based on the “infinite-site” theory (Fig. S3; see  
337 Section 2.6 in Supplemental Methods) we were able to select the most precise estimates  
338 of *Prochlorococcus* evolutionary timeline for illustration (Fig. S6) and further discussion.

339 Evolution of genome content via gene gains and losses was inferred using two  
340 independent methods, AnGST<sup>66</sup> and BadiRate v1.35<sup>67</sup>. The former assumes that the  
341 statistically supported topological differences between a gene tree and the species tree  
342 result from evolutionary events (gene loss, gene duplication, HGT, gene birth and  
343 speciation), and infers these evolutionary events by reconciling the topological  
344 incongruences under a generalized parsimony framework by achieving a minimum

345 number of the evolutionary events along the species tree, with penalties of an  
346 evolutionary event determined by the genome flux analysis (Fig. S7)<sup>66</sup>. The latter does  
347 not rely on the tree topological incongruence information, but instead uses a full  
348 maximum-likelihood approach to determine the gene family turnover rates that  
349 maximizes the probability of observing the gene count patterns provided by the family  
350 size table. The BadiRate analyses were run using nine strategies each with a distinct  
351 turnover rate model and a distinct branch model. The likelihoods of different runs were  
352 compared (Fig. S8), and three strategies with highest likelihood values were used (Fig.  
353 S9). Further, results derived from AnGST (Fig. S10) and BadiRate were compared and  
354 summarized to determine the common patterns shared by the two software (Fig. S11),  
355 and important functional genes discussed were consistently inferred by these two  
356 methods. As the two methods inferred the qualitatively same pattern of genome size  
357 reduction on the branches leading to SBE-LCA, the number of gene gains and losses  
358 derived from the AnGST analysis was presented.

359 The inference of a potential change of selection efficiency on a given branch was  
360 performed by comparing the genome-wide  $d_R/d_C$  value across single-copy orthologous  
361 genes of the branch to that of the closest sister branch. The  $d_R/d_C$  value was calculated  
362 using RCCalculator (<http://www.geneorder.org/RCCalculator/>; see Section 4 in  
363 Supplemental Methods) based on two independent amino acid classification schemes  
364 (Table S5).

365



## 366 References

- 367 1 Biller, S. J., Berube, P. M., Lindell, D. & Chisholm, S. W. Prochlorococcus: the structure  
368 and function of collective diversity. *Nat Rev Microbiol* **13**, 13 (2015).
- 369 2 Johnson, Z. I. *et al.* Niche partitioning among Prochlorococcus ecotypes along ocean-scale  
370 environmental gradients. *Science (80- )* **311**, 1737-1740 (2006).
- 371 3 West, N. J. & Scanlan, D. J. Niche-partitioning of Prochlorococcus populations in a  
372 stratified water column in the eastern North Atlantic Ocean. *Appl Environ Microbiol* **65**,  
373 2585-2591 (1999).
- 374 4 Hess, W. R. *et al.* The photosynthetic apparatus of Prochlorococcus: insights through  
375 comparative genomics. *Photosynth Res* **70**, 53-71 (2001).
- 376 5 Moore, L. R., Rocap, G. & Chisholm, S. W. Physiology and molecular phylogeny of  
377 coexisting Prochlorococcus ecotypes. *Nature* **393**, 464 (1998).
- 378 6 Batut, B., Knibbe, C., Marais, G. & Daubin, V. Reductive genome evolution at both ends  
379 of the bacterial population size spectrum. *Nat Rev Microbiol* **12**, 841 (2014).
- 380 7 Luo, H., Friedman, R., Tang, J. & Hughes, A. L. Genome reduction by deletion of paralogs  
381 in the marine cyanobacterium Prochlorococcus. *Mol Biol Evol* **28**, 2751-2760 (2011).
- 382 8 Hu, J. & Blanchard, J. L. Environmental sequence data from the Sargasso Sea reveal that  
383 the characteristics of genome reduction in Prochlorococcus are not a harbinger for an  
384 escalation in genetic drift. *Mol Biol Evol* **26**, 5-13 (2008).
- 385 9 Luo, H., Huang, Y., Stepanauskas, R. & Tang, J. Excess of non-conservative amino acid  
386 changes in marine bacterioplankton lineages with reduced genomes. *Nat Microbiol* **2**,  
387 17091 (2017).
- 388 10 Zuckerkandl, E. P., Linus. in *Evolving genes and proteins* 97-166 (Elsevier, 1965).
- 389 11 Dayhoff, M. O. A model of evolutionary change in proteins. *Atlas of protein sequence and*  
390 *structure* **5**, 89-99 (1972).
- 391 12 Falkowski, P. G., Fenchel, T. & Delong, E. F. The microbial engines that drive Earth's  
392 biogeochemical cycles. *Science (80- )* **320**, 1034-1039 (2008).
- 393 13 Kettler, G. C. *et al.* Patterns and implications of gene gain and loss in the evolution of  
394 Prochlorococcus. *PLoS Genet* **3**, e231 (2007).
- 395 14 Sánchez-Baracaldo, P. Origin of marine planktonic cyanobacteria. *Sci Rep* **5**, 17418 (2015).
- 396 15 Sánchez-Baracaldo, P., Ridgwell, A. & Raven, J. A. A neoproterozoic transition in the  
397 marine nitrogen cycle. *Current Biology* **24**, 652-657 (2014).
- 398 16 Marshall, C. R. Using the Fossil Record to Evaluate Timetree Timescales. *Front Genet* **10**,  
399 1049 (2019).
- 400 17 Di Rienzi, S. C. *et al.* The human gut and groundwater harbor non-photosynthetic bacteria  
401 belonging to a new candidate phylum sibling to Cyanobacteria. *Elife* **2**, e01102 (2013).
- 402 18 Soo, R. M., Hemp, J., Parks, D. H., Fischer, W. W. & Hugenholtz, P. On the origins of  
403 oxygenic photosynthesis and aerobic respiration in Cyanobacteria. *Science (80- )* **355**,  
404 1436-1440 (2017).
- 405 19 Hoffman, P. F., Kaufman, A. J., Halverson, G. P. & Schrag, D. P. A Neoproterozoic  
406 snowball earth. *Science (80- )* **281**, 1342-1346 (1998).
- 407 20 Ashkenazy, Y. *et al.* Dynamics of a Snowball Earth ocean. *Nature* **495**, 90 (2013).
- 408 21 Zinser, E. R. *et al.* Influence of light and temperature on Prochlorococcus ecotype  
409 distributions in the Atlantic Ocean. *Limnol Oceanogr* **52**, 2205-2220 (2007).
- 410 22 Thomas, D. & Dieckmann, G. Antarctic sea ice--a habitat for extremophiles. *Science (80- )*  
411 **295**, 641-644 (2002).
- 412 23 Hoffman, P. F. *et al.* Snowball Earth climate dynamics and Cryogenian geology-geobiology.  
413 *Sci Adv* **3**, e1600983 (2017).

- 414 24 Takeuchi, N. Optical characteristics of cryoconite (surface dust) on glaciers: the  
415 relationship between light absorbency and the property of organic matter contained in the  
416 cryoconite. *Annals of Glaciology* **34**, 409-414 (2002).
- 417 25 Benforte, F. C. *et al.* Novel role of the LPS core glycosyltransferase WapH for cold  
418 adaptation in the Antarctic bacterium *Pseudomonas extremaustralis*. *PLoS One* **13**,  
419 e0192559 (2018).
- 420 26 Wang, Z., Wang, J., Ren, G., Li, Y. & Wang, X. Influence of core oligosaccharide of  
421 lipopolysaccharide to outer membrane behavior of *Escherichia coli*. *Mar Drugs* **13**, 3325-  
422 3339 (2015).
- 423 27 Feller, G. & Gerday, C. Psychrophilic enzymes: hot topics in cold adaptation. *Nat Rev*  
424 *Microbiol* **1**, 200 (2003).
- 425 28 Uhde, A. *et al.* Glucosamine as carbon source for amino acid-producing *Corynebacterium*  
426 *glutamicum*. *Appl Microbiol Biotechnol* **97**, 1679-1687 (2013).
- 427 29 Park, J. T. & Uehara, T. How Bacteria Consume Their Own Exoskeletons (Turnover and  
428 Recycling of Cell Wall Peptidoglycan). *Microbiology and Molecular Biology Reviews* **72**,  
429 211-227 (2008).
- 430 30 Borisova, M. *et al.* Peptidoglycan Recycling in Gram-Positive Bacteria Is Crucial for  
431 Survival in Stationary Phase. *MBio* **7** (2016).
- 432 31 Schumann, W. Regulation of bacterial heat shock stimulons. *Cell Stress and Chaperones*  
433 **21**, 959-968 (2016).
- 434 32 La Terza, A., Papa, G., Miceli, C. & Luporini, P. Divergence between two Antarctic species  
435 of the ciliate *Euplotes*, *E. focardii* and *E. nobilii*, in the expression of heat-shock protein 70  
436 genes. *Mol Ecol* **10**, 1061-1067 (2001).
- 437 33 Rinehart, J. P. *et al.* Continuous up-regulation of heat shock proteins in larvae, but not  
438 adults, of a polar insect. *Proc Natl Acad Sci U S A* **103**, 14223-14227 (2006).
- 439 34 Lawrence, R. P. & William, J. W. Temperature and substrates as interactive limiting factors  
440 for marine heterotrophic bacteria. *Aquatic Microbial Ecology* **23**, 187-204 (2001).
- 441 35 Gleitz, M., v.d. Loeff, M. R., Thomas, D. N., Dieckmann, G. S. & Millero, F. J. Comparison  
442 of summer and winter inorganic carbon, oxygen and nutrient concentrations in Antarctic  
443 sea ice brine. *Mar Chem* **51**, 81-91 (1995).
- 444 36 Reay, D. S., Nedwell, D. B., Priddle, J. & Ellis-Evans, J. C. Temperature dependence of  
445 inorganic nitrogen uptake: reduced affinity for nitrate at suboptimal temperatures in both  
446 algae and bacteria. *Appl. Environ. Microbiol.* **65**, 2577-2584 (1999).
- 447 37 Raven, J. A., Wollenweber, B. & Handley, L. L. A comparison of ammonium and nitrate as  
448 nitrogen sources for photolithotrophs. *New Phytologist* **121**, 19-32 (1992).
- 449 38 Webster-Brown, J. G., Hawes, I., Jungblut, A. D., Wood, S. A. & Christenson, H. K. The  
450 effects of entombment on water chemistry and bacterial assemblages in closed cryoconite  
451 holes on Antarctic glaciers. *FEMS Microbiol Ecol* **91** (2015).
- 452 39 Mao, X. *et al.* Computational prediction of the osmoregulation network in *Synechococcus*  
453 *sp.* WH8102. *BMC Genomics* **11**, 291 (2010).
- 454 40 Scanlan, D. J. *et al.* Ecological genomics of marine picocyanobacteria. *Microbiol. Mol.*  
455 *Biol. Rev.* **73**, 249-299 (2009).
- 456 41 Empadinhas, N. & da Costa, M. S. To be or not to be a compatible solute: bioversatility of  
457 mannosylglycerate and glucosylglycerate. *Syst Appl Microbiol* **31**, 159-168 (2008).
- 458 42 Carver, J. H. & Vardavas, I. M. Precambrian glaciations and the evolution of the  
459 atmosphere. *Ann Geophys* **12**, 674-682 (1994).
- 460 43 Raven, J. A., Kübler, J. & Beardall, J. Put out the light, and then put out the light. *Journal*  
461 *of the Marine Biological Association of the United Kingdom* **80**, 1-25 (2000).
- 462 44 Simon, C., Wiezer, A., Strittmatter, A. W. & Daniel, R. Phylogenetic diversity and

- 463 metabolic potential revealed in a glacier ice metagenome. *Appl Environ Microbiol* **75**,  
464 7519-7526 (2009).
- 465 45 Kouril, R., Wientjes, E., Bultema, J. B., Croce, R. & Boekema, E. J. High-light vs. low-  
466 light: effect of light acclimation on photosystem II composition and organization in  
467 *Arabidopsis thaliana*. *Biochimica et Biophysica Acta (BBA)-Bioenergetics* **1827**, 411-419  
468 (2013).
- 469 46 Bibby, T., Mary, I., Nield, J., Partensky, F. & Barber, J. Low-light-adapted *Prochlorococcus*  
470 species possess specific antennae for each photosystem. *Nature* **424**, 1051 (2003).
- 471 47 Dong, G. & Golden, S. S. How a cyanobacterium tells time. *Curr Opin Microbiol* **11**, 541-  
472 546 (2008).
- 473 48 Holtzendorff, J. *et al.* Genome streamlining results in loss of robustness of the circadian  
474 clock in the marine cyanobacterium *Prochlorococcus marinus* PCC 9511. *J Biol Rhythms*  
475 **23**, 187-199 (2008).
- 476 49 Axmann, I. M. *et al.* Biochemical evidence for a timing mechanism in *prochlorococcus*. *J*  
477 *Bacteriol* **191**, 5342-5347 (2009).
- 478 50 Mella-Flores, D. *et al.* *Prochlorococcus* and *Synechococcus* have Evolved Different  
479 Adaptive Mechanisms to Cope with Light and UV Stress. *Front Microbiol* **3**, 285 (2012).
- 480 51 Giovannoni, S. J., Thrash, J. C. & Temperton, B. Implications of streamlining theory for  
481 microbial ecology. *ISME J* **8**, 1553 (2014).
- 482 52 Warters, R. L. & Lyons, B. W. Variation in radiation-induced formation of DNA double-  
483 strand breaks as a function of chromatin structure. *Radiat Res* **130**, 309-318 (1992).
- 484 53 Simons, M. J. The evolution of the cyanobacterial posttranslational clock from a primitive  
485 “phoscillator”. *J Biol Rhythms* **24**, 175-182 (2009).
- 486 54 Mullineaux, C. W. & Stanewsky, R. The rolex and the hourglass: a simplified circadian  
487 clock in *Prochlorococcus*? *J Bacteriol* **191**, 5333-5335 (2009).
- 488 55 Moczyłowska, M. The Ediacaran microbiota and the survival of Snowball Earth  
489 conditions. *Precambrian Res* **167**, 1-15 (2008).
- 490 56 Hoffman, P. F. & Schrag, D. P. The snowball Earth hypothesis: testing the limits of global  
491 change. *Terra nova* **14**, 129-155 (2002).
- 492 57 Allison, C. W. & Awramik, S. M. Organic-walled microfossils from earliest Cambrian or  
493 latest Proterozoic Tindir Group rocks, northwest Canada. *Precambrian Res* **43**, 253-294  
494 (1989).
- 495 58 Corsetti, F. A., Awramik, S. M. & Pierce, D. A complex microbiota from snowball Earth  
496 times: microfossils from the Neoproterozoic Kingston Peak Formation, Death Valley, USA.  
497 *Proc Natl Acad Sci USA* **100**, 4399-4404 (2003).
- 498 59 Olcott, A. N., Sessions, A. L., Corsetti, F. A., Kaufman, A. J. & De Oliviera, T. F. Biomarker  
499 evidence for photosynthesis during Neoproterozoic glaciation. *Science (80- )* **310**, 471-474  
500 (2005).
- 501 60 Yang, Z. PAML 4: phylogenetic analysis by maximum likelihood. *Mol Biol Evol* **24**, 1586-  
502 1591 (2007).
- 503 61 Battistuzzi, F. U. & Hedges, S. B. A major clade of prokaryotes with ancient adaptations to  
504 life on land. *Mol Biol Evol* **26**, 335-343 (2008).
- 505 62 Shih, P. M. *et al.* Improving the coverage of the cyanobacterial phylum using diversity-  
506 driven genome sequencing. *Proc Natl Acad Sci USA* **110**, 1053-1058 (2013).
- 507 63 Blank, C. & Sanchez-Baracaldo, P. Timing of morphological and ecological innovations in  
508 the cyanobacteria—a key to understanding the rise in atmospheric oxygen. *Geobiology* **8**, 1-  
509 23 (2010).
- 510 64 Uyeda, J. C., Harmon, L. J. & Blank, C. E. A comprehensive study of cyanobacterial  
511 morphological and ecological evolutionary dynamics through deep geologic time. *PLoS*

512 *One* **11**, e0162539 (2016).  
513 65 Schirrmeister, B. E., Sanchez-Baracaldo, P. & Wacey, D. Cyanobacterial evolution during  
514 the Precambrian. *Int J Astrobiol* **15**, 187-204 (2016).  
515 66 David, L. A. & Alm, E. J. Rapid evolutionary innovation during an Archaean genetic  
516 expansion. *Nature* **469**, 93 (2011).  
517 67 Librado, P., Vieira, F. & Rozas, J. BadiRate: estimating family turnover rates by likelihood-  
518 based methods. *Bioinformatics* **28**, 279-281 (2011).  
519

520 **Acknowledgments**

521           We thank Allison Coe, Erik Zinser, and Zackary Johnson for providing the data of  
522 *Prochlorococcus* growth rates, Sishuo Wang, Tianhua Liao and Xiaoyuan Feng for their  
523 suggestions on molecular dating analyses. This work is supported by the National Natural  
524 Science Foundation of China (92051113), the Hong Kong Research Grants Council  
525 General Research Fund (14110820), the Hong Kong Research Grants Council Area of  
526 Excellence Scheme (AoE/M-403/16), HKU FoS funds to SAC, and the Direct Grant of  
527 CUHK (4053257 and 3132809).

528

529 **Author Contributions**

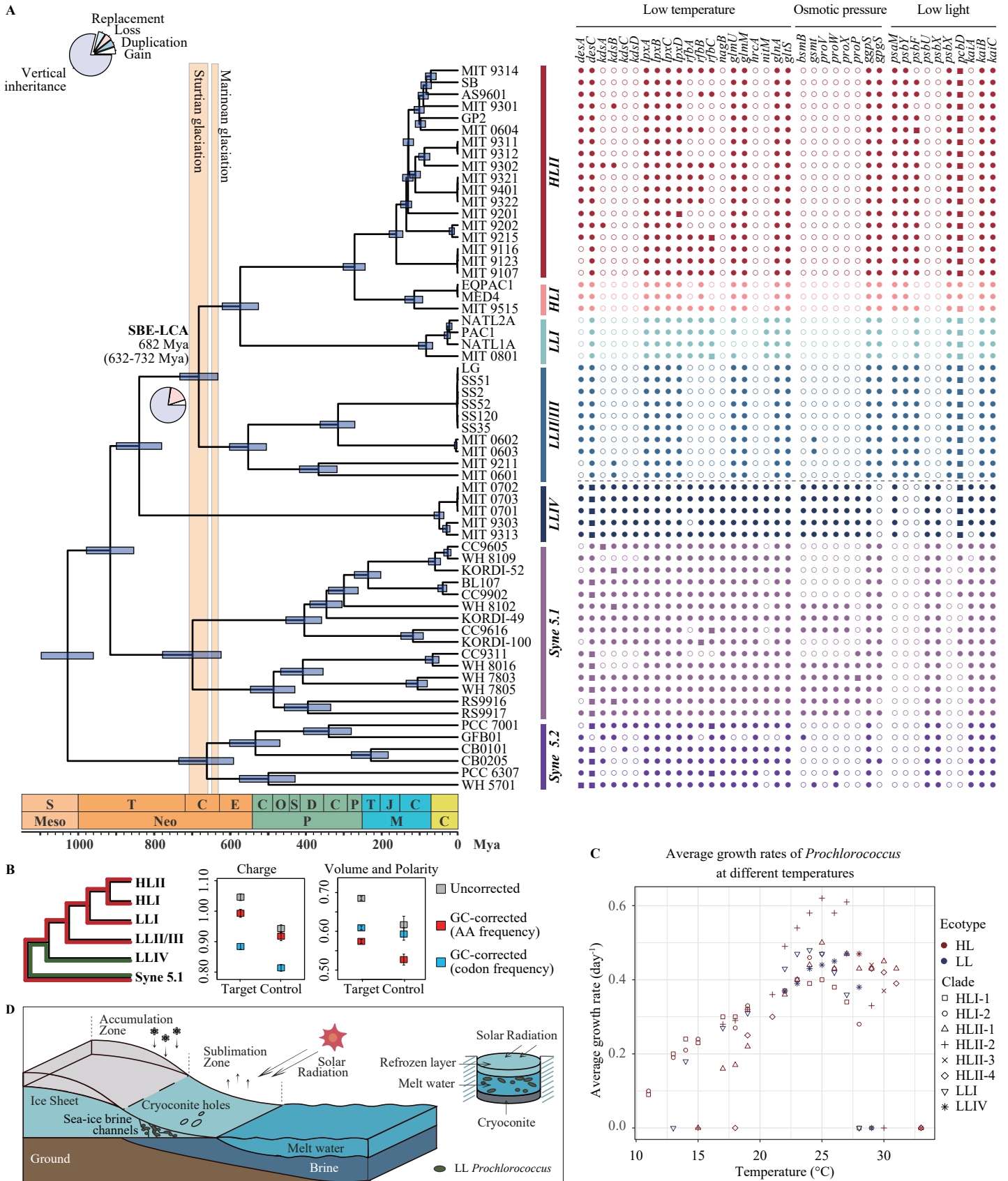
530           H.L. conceived and directed the study. H.Z. and Y.S. performed the  
531 bioinformatics. All authors contribute to the interpretation of the results. H.Z., Y.S.,  
532 S.A.C and H.L. wrote the paper.

533

534 **Conflict of interests**

535           The author declares no competing interests.

**Fig. 1**



536 Fig. 1 Evolution of *Prochlorococcus* during the Neoproterozoic Snowball Earth events.

537 (A) (Left) Chronogram of the evolutionary history of *Prochlorococcus* estimated by

538 MCMCTree. The evolutionary tree shown here is part of the species tree constructed with

539 MrBayes based on 90 compositionally homogenous gene families shared by 159

540 cyanobacterial genomes (Fig. S4 D). Divergence time is estimated based on 27 gene

541 sequences under calibration set C9 (Table S1). The vertical bars represent the estimated

542 time of the Neoproterozoic glaciation events. The flanking horizontal blue bars on

543 ancestral nodes represent the posterior 95% highest probability density (HPD) interval of

544 the estimated divergence time. The pie chart on the ancestral branches leading to the node

545 SBE-LCA provides the proportion of reconstructed genomic events including gene gain,

546 gene loss, gene replacement, gene duplication and gene vertical inheritance. (Right)

547 Phyletic pattern of key gene families that potentially enabled *Prochlorococcus* to survive

548 harsh conditions during the Neoproterozoic Snowball Earth (at the ancestral node ‘SBE-

549 LCA’). Solid square, solid circle and open circle next to each extant taxon represent

550 multi-copy gene family, single-copy gene family, and absence of the gene family,

551 respectively, in the genome. (B) (Left) The diagram helps understand how the  $d_R/d_C$  was

552 calculated. In this context, the ‘Target’ group includes all genomes of all HL clades, LLI

553 and LLII/III, the ‘Control’ group includes all genomes of LLIV, and the ‘reference’

554 group includes all genomes of Syne 5.1. The  $d_R/d_C$  for the ‘Target’ group (shown in

555 Middle & Right) is calculated by comparing a genome from the ‘Target’ group to a

556 genome from the ‘reference’ group (marked with red), followed by averaging the value

557 across all possible genome pairs. Likewise, the  $d_R/d_C$  for the ‘Control’ group (shown in

558 Middle & Right) is calculated by comparing a genome from the ‘Control’ group to a

559 genome from the ‘reference’ group (marked with green) and then by averaging the value  
560 across all possible genome pairs. (Middle & Right) The genome-wide means of  $d_R/d_C$   
561 values at the ancestral branch leading to SBE-LCA and that at its sister lineage. They  
562 were classified based on the physicochemical classification of the amino acids by charge  
563 or by volume and polarity, and were either GC-corrected by codon frequency (blue), GC-  
564 corrected by amino acid (AA) frequency (red) or uncorrected (gray). Error bars of  $d_R/d_C$   
565 values represent the standard error of the mean. (C) Diagram of putative bacterial refugia  
566 including cryoconite holes and sea ice brine channels in Neoproterozoic Snowball Earth,  
567 which were featured with a number of stresses such as low temperature, low light, and  
568 variable osmotic pressure. (D) The average growth rate of *Prochlorococcus* ecotypes at  
569 different temperatures. Replicate cell cultures were grown in a 14:10 light: dark cycle at  
570  $66 \pm 1 \mu\text{mol m}^{-2}\text{s}^{-1}$ . The growth data used for plotting are collected from Johnson et al.  
571 2006 and Zinser et al. 2007.